Journal of Power Sources 186 (2009) 393–398

Contents lists available at ScienceDirect

Journal of Power Sources

journal homepage: www.elsevier.com/locate/jpowsour

Catalyst layer-free carbon-coated steel—An easy route to bipolar plates of polymer electrolyte membrane fuel cells: Characterization on structure and electrochemistry

Chih-Yeh Chung[a], Shi-Kun Chen[a,*], Tsung-Shune Chin[a,b], Tse-Hao Ko[a], Shiuan-Wen Lin[a], Wei-Min Chang[a], Shih-Nan Hsiao[a]

[a] Department of Materials Science and Engineering, Feng Chia University, Taichung 40724, Taiwan
[b] Department of Engineering and System Science, National Tsing Hua University, Hsichu 300, Taiwan

ARTICLE INFO

Article history:
Received 1 September 2008
Received in revised form 2 October 2008
Accepted 2 October 2008
Available online 22 October 2008

Keywords:
Metallic bipolar plate
Carbon coating
Interfacial contact resistance
Hydrophobicity
Chemical stability

ABSTRACT

Stainless steel coated with carbon by CVD process has been evaluated as a low-cost and small-volume substitute for graphite bipolar plate in polymer electrolyte membrane fuel cell (PEMFC). Carbon film was grown at 690–930 °C under gas-mixture of C_2H_2–H_2. Scanning electron microscopy and X-ray diffractometry were used to characterize surface morphology and crystal structure of resultant carbon films, which were found to depend much on reaction temperature. Interfacial contact resistance (ICR), hydrophobicity and chemical stability of obtained specimens were measured to compare with commercial highly oriented pyrolytic graphite (HOPG). All carbon films investigated in this study show improved ICR and hydrophobicity of SUS304 substrate to the level of HOPG. Amorphous carbon layer with continuous film structure prepared at 810 °C shows the best protection of SUS304 substrate against the attack of $H_{(aq)}^+$ (anodic side) and the best resistance of the coated carbon from gasification (cathodic side) in the simulated PEMFC environment.

1. Introduction

Oil crisis and environment protection have raised great concern in recent years to develop alternative energies. Polymer electrolyte membrane fuel cell (PEMFC), as one of the potential substitutes, is a kind of high-efficiency power generator with no pollutant by-products [1]. So far the reason why PEMFC has not yet been extensively used is due to its high cost and huge volume. Improvement in bipolar plate is a good solution since bipolar plate constitutes about 29% cost and 95% volume of PEMFC [2]. Graphite and carbon composite are conventional materials for bipolar plate because of their excellent chemical stability. However, graphite is expensive in both material cost and machining of gas channels; carbon composite shows poor electric conductivity as a result of polymer resin as the matrix [3,4]. In both case, the need of a sufficient thickness to redeem poor mechanical strength as well as to prevent fuel leakage (notably hydrogen) handicaps miniaturization of PEMFC.

Metallic plates are hopeful alternates to graphite plate by virtue of their promising properties in terms of mechanical strength, electric conductivity, and gas-tightness [5–7]. Shaping gas channels thereon is relatively easy and cheap. Nevertheless, metallic plates perform disappointingly in interfacial contact resistance (ICR), hydrophobicity, and chemical stability. Each of these factors decreases power output of PEMFC, specifically chemical stability [8]. Alloys with special compositions and surface modification have been investigated intensively to improve the performance of metallic bipolar plate. A novel approach integrating advantages of carbon and metal is to deposit a carbon film onto a metallic bipolar plate, thus said to alleviate shortcomings of metallic bipolar plate described above. But the deposited carbon was fibrous [9] or less chemically stable as compared with commercial graphite [10,11].

In our prior study carbon film was deposited onto Ni-coated stainless steel SUS304 (approximately, in wt.%: 70.2% Fe, 18.7% Cr, and 8.4% Ni) by chemical vapor deposition (CVD) under acetylene–hydrogen mixed gas atmosphere [12]. Ni layer in this case behaves as a catalyst to promote graphitization of carbon adatoms [13,14]. The Ni-catalyzed carbon film exhibits mirror-like smoothness and excellent electric conductivity. Its most impressive function is a promising protection of SUS304 bipolar plate by a corrosion endurance test in 0.5 M H_2SO_4 solution and by a performance reliability test after 100 h PEMFC operation. In the current study carbon film was directly deposited on bare SUS304 plate without a Ni-catalytic layer, extremely difficult but much cheaper and time

* Corresponding author. Tel.: +886 4 24512298; fax: +886 4 24510014.
E-mail address: skchen@fcu.edu.tw (S.-K. Chen).

0378-7753/$ – see front matter © 2008 Elsevier B.V. All rights reserved.
doi:10.1016/j.jpowsour.2008.10.047

budget as compared with Ni-catalyzed one. The resultant carbon film performs satisfactorily in aspects of ICR, hydrophobicity, and much superior in chemical stability than our previous carbon coating and commercial highly oriented pyrolytic graphite (HOPG), as to be disclosed thereinafter.

2. Experimental

2.1. Preparation and characterization of carbon film

Polished SUS304 stainless steel plates (20 mm × 20 mm × 1 mm) were placed in a tube furnace to deposit carbon film by CVD method at 690–930 °C under acetylene–hydrogen mixed gas atmosphere (mixing ratio of C_2H_2/H_2 is 0.6). During heating up to reaction temperature or cooling down to ambient temperature, specimens were processed under a hydrogen-containing atmosphere. Scanning electron microscope (SEM) was used to observe surface morphologies of the obtained specimens. Crystal structure of the prepared carbon films was identified by grazing incident X-ray diffraction at a grazing angle $\theta = 3^\circ$. ICRs between obtained specimens and carbon paper (TGPH090, Toray) were measured with a milliohm-meter (4338B, Agilent) by a sandwich method [6]. Hydrophobicity of each specimen surface was analyzed by a sessile drop method using distilled water droplets. In our experiments commercial HOPG (AXF-5QCF, Poco) ground with 4000-grit sandpaper was used as the control.

2.2. Electrochemical stability tests

Chemical tests were carried out at 25 °C via a potentiodynamic polarization technique in an undivided three-electrode glass cell (250 cm^3 in volume) with an auxiliary electrode Pt mesh (110 cm^2) and a reference electrode Ag/AgCl (saturated KCl). Specimens (working electrodes) were mounted on this cell and subjected to an accelerated corrosion test in which 0.5 M H_2SO_4 solution (pH 0.4) was used to simulate severer corrosion conditions inside PEMFC. Potentiodynamic polarization curves were recorded with a potentiostat (model 6081C, CHI) at a scan rate 10 mV s^{-1} from −0.80 to 2.20 V_{RHE} (V_{RHE} is the potential of reversible hydrogen electrode, RHE). After chemical stability tests, concentrations of metal ions in each H_2SO_4 solution were gauged with an inductively coupled-plasma atomic emission spectrometer (ICP-AES).

3. Results and discussion

3.1. Influence of CVD reaction temperature on morphology of carbon deposits

Fig. 1 shows three typical morphologies of carbon films on polished SUS304 substrates obtained by changing CVD temperature (T_{CVD}). Carbon filaments, 100–150 nm in diameter, form on specimen surface at T_{CVD} 690 °C as shown in Fig. 1(a). At T_{CVD} 810–930 °C, a continuous film structure develops on specimen surface instead of carbon filaments. Film surface is characterized by spherical carbon granules, whose diameter spans from 0.7 to 2.5 μm with increasing T_{CVD}. Carbon beads over 1 μm diameter as manifested in Fig. 1(c) also form at higher reaction temperature, such as 930 °C. They exhibit poor adhesion to carbon film.

Prior studies indicated that pyrolytic carbon molecules form graphitic carbon layer through the catalysis of catalytic metal beneath. Interspaces between graphite (0 0 2) planes non-parallel to film surface provide paths for metal atoms to migrate from metal layer until the top of carbon film. Metal atoms coalesce to small particles on the top and subsequently catalyze carbon adatoms to carbon filaments [15]. On the contrary, metal atoms fail to reach the top if their migration velocity is slower than growth velocity of carbon film. In this case carbon deposit tends to form a continuous film structure rather than carbon filaments [12]. Of particular interest is our CVD process at T_{CVD} 690 °C leads to carbon filaments and continuous film structure on SUS304 substrate without and with a Ni-coating, respectively. We reasonably attribute the above phenomenon to the different migration velocities of Ni and Fe atoms, since Fe constitutes over 70 at.% of SUS304. Unlike Ni, Fe is able to form metastable carbide in graphitization process [15,16], offering

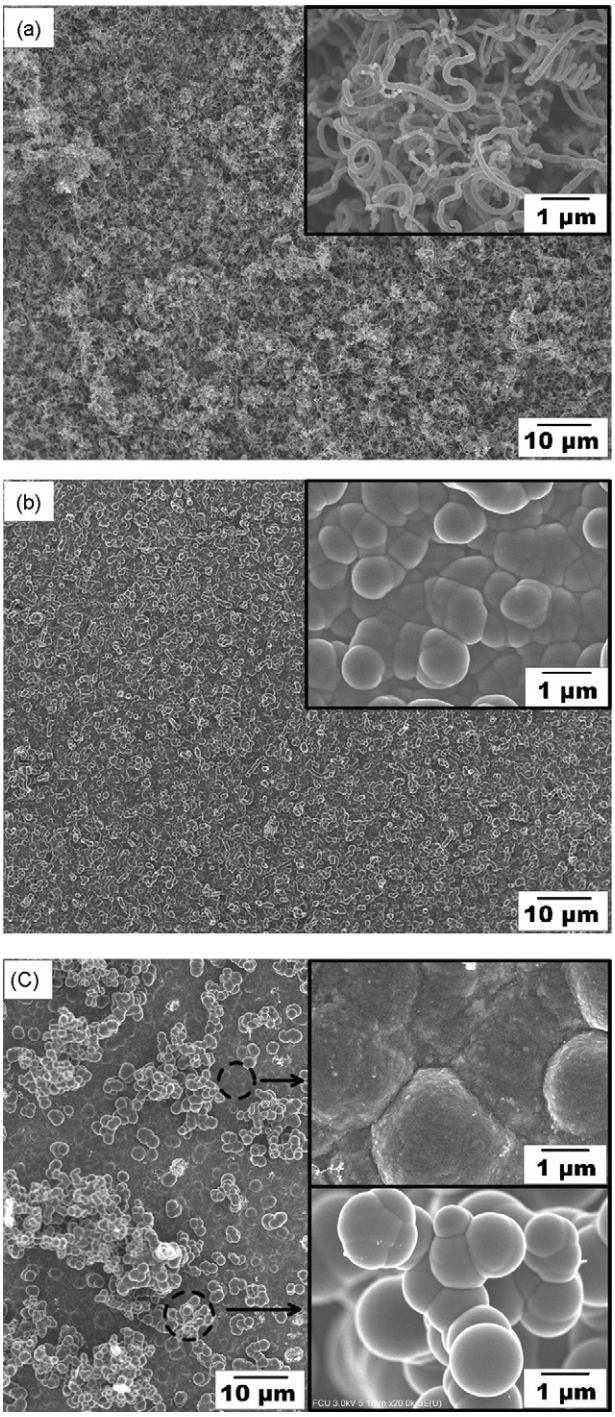

Fig. 1. SEM images of the surface morphology of the specimens prepared at (a) 690 °C, (b) 810 °C and (c) 930 °C.

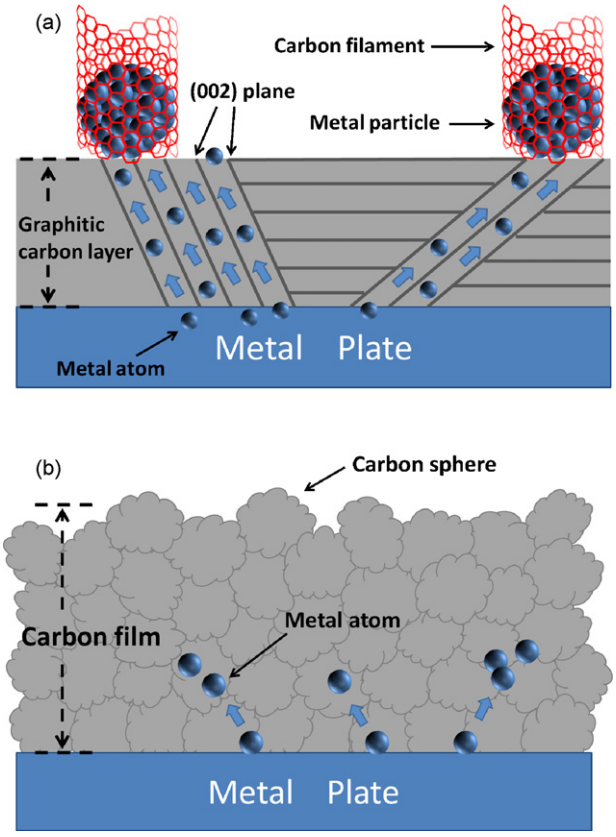

Fig. 2. Schematic representation of the developments of (a) carbon filament and (b) continuous film structure.

another path for Fe atoms to migrate rapidly. Fe atoms therefore reach the top more readily and induce growth of carbon filaments at this 'lower' temperature of our CVD process.

In our CVD process, a great deal of pyrolytic carbon spheres form as T_{CVD} is high enough. The development of carbon films on specimens prepared at T_{CVD} 810–930 °C is basically through the accumulation of carbon spheres. This also interprets why growth velocities of these carbon films at high temperatures are rapid enough to prevent the formation of Fe-catalyzed carbon filaments. Development mechanisms of carbon filament and continuous film structure are schematically illustrated in Fig. 2(a) and (b), respectively.

3.2. Structure analyses

X-ray diffraction patterns of specimens grown at different T_{CVD} are shown in Fig. 3, in which the dash line is (0 0 2) diffraction line of HOPG. 690 °C-prepared carbon film displays a relatively obvious (0 0 2) diffraction peak which shifts to lower angle as compared with the dash line, demonstrating that d_{002}-spacing of 690 °C-prepared carbon film is larger than that of HOPG. This stems from the strain induced by bending graphenes which roll up into tubular shape in carbon filament structure [17]. 810 °C-prepared carbon film displays indistinct diffraction peaks, implying it is amorphous in nature. 870 °C- and 930 °C-prepared ones display manifest graphite (0 0 2) diffraction peaks whose full width at half maximum decreases, i.e. degree of graphitic ordering increases, as T_{CVD} is raised.

Continuous carbon film structure prepared at T_{CVD} 810–930 °C, as mentioned above, consists of pyrolytic carbon spheres. According to Inagaki's study, small-sized pyrolytic carbon spheres

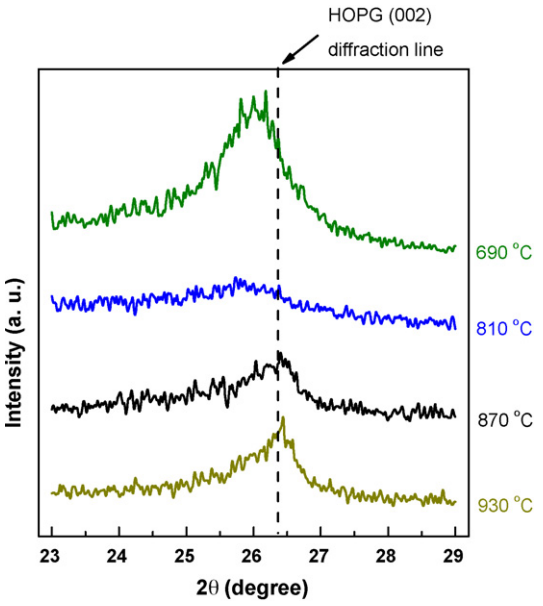

Fig. 3. X-ray diffraction patterns of specimens prepared at 690, 810, 870, and 930 °C, respectively.

(30–500 nm in diameter) are amorphous in structure, whereas large-sized ones (1–2 μm in diameter) show high degree of graphitic ordering [18,19]. Here, we deduce that amorphous structure of 810 °C-prepared carbon film arises from the accumulation of small-sized carbon spheres as manifested in Fig. 1(b). On the contrary, many carbon beads of over 1 μm diameter form at T_{CVD} 930 °C (Fig. 1(c)), whereupon the underneath film is likely composed of large-sized carbon spheres, being consistent with the appearance of sharper graphite (0 0 2) diffraction peak observed in Fig. 3. Random arrangement of these spheres in carbon film induces small coherency of graphite phase, which interprets why graphite (0 0 2) diffraction peak of 930 °C-prepared carbon film is still broad in full width at half maximum.

3.3. Interfacial contact resistance (ICR)

ICR between metallic bipolar plate and gas diffusion layer is a critical factor in the internal impedance of PEMFC stack. Fig. 4 shows the ICR of each specimen to gas diffusion layer (carbon paper) as

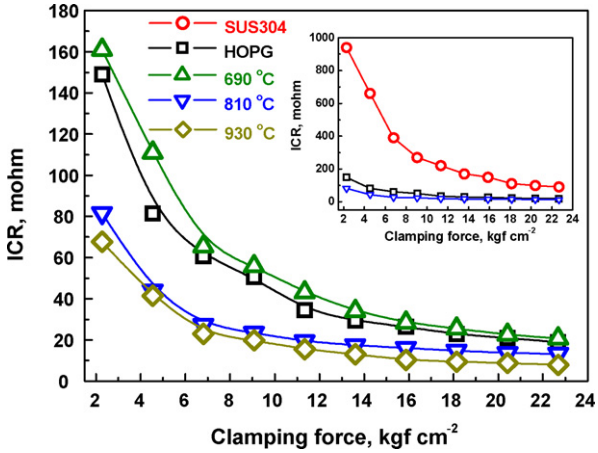

Fig. 4. Variation of interfacial contact resistance with clamping force for bare stainless steel, HOPG and specimens prepared at 690–930 °C.

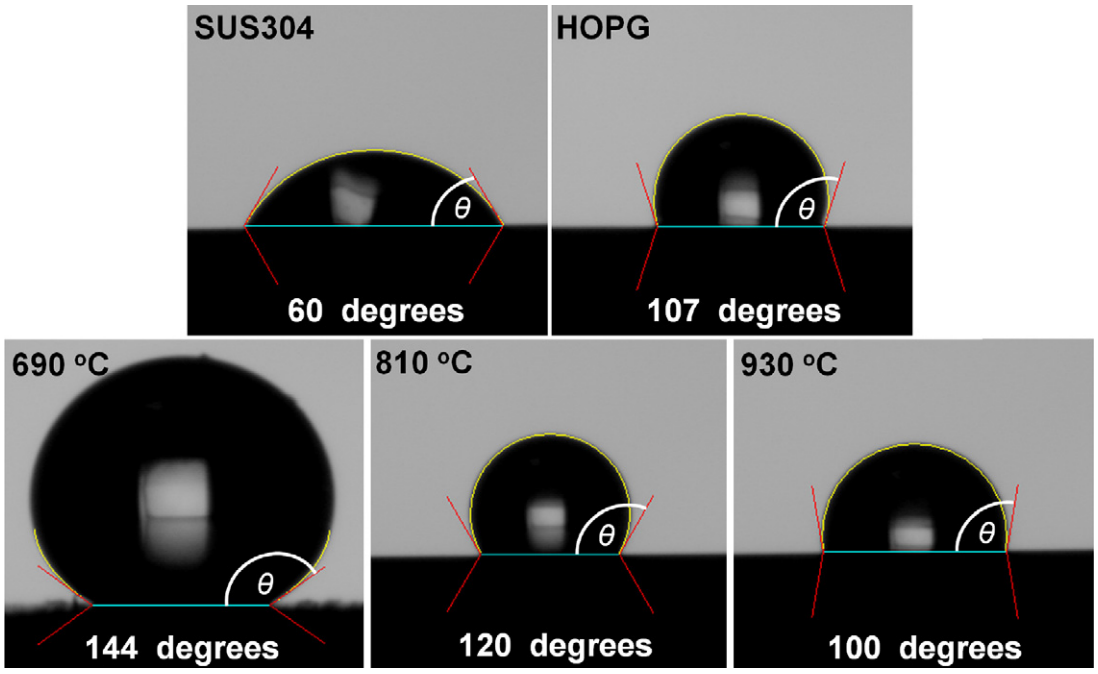

Fig. 5. Images of distilled water droplets on the surface of investigated specimens.

a function of clamping force. 690 °C-prepared specimen performs quite closely to HOPG in ICR though a little inferior; while 810 °C- and 930 °C-prepared ones perform much better. The disadvantage of 690 °C-prepared specimen results from its porous surface composed of carbon filaments, which decreases the contact area between the specimen and carbon paper. Compared with 810 °C-prepared specimen, the lower ICR of 930 °C-prepared one arises from its more graphitic film structure, leading to better electric conductivity. The inset graph in Fig. 4 depicts that for bare SUS304 the ICR is much larger than those of other carbon-coated specimens at low clamping force. The high ICR is most likely caused by the surface passivation layer of stainless steel [20,21].

810 °C- and 930 °C-prepared specimens show ICRs of 81.7 mΩ and 67.7 mΩ, respectively, under a clamping force of 2.3 kgf cm^{-2}, both are smaller than that of bare SUS304 plate (90.7 mΩ) under a 10-times-larger clamping force (23 kgf cm^{-2}). These results prove the fact that strong clamping force is no longer essential for reducing internal impedance of PEMFC with our carbon-coated metallic bipolar plate. This brings two benefits from the much smaller clamping force. First is the decrease in PEMFC volume due to the adoptability of thinner coated metallic bipolar plate without the deformation of PEMFC assembly unit. Second is the improved PEMFC performance by alleviating the deformation of gas diffusion layer, since a deformed gas diffusion layer shows poor porosity which increases resistance to gas transport and may result in water flooding [22].

3.4. Hydrophobicity

Bipolar plate with poor hydrophobicity delays drainage of produced water from its gas channels, which eventuates in accumulation of water and consequent flooding in PEMFC. Fig. 5 shows measurement results of contact angle between a water droplet and different substrates. Generally speaking, a hydrophobic material exhibits a contact angle more than 90° between liquid–vapor and liquid–solid surfaces as a water droplet is placed onto its surface. In Fig. 5, a polished SUS304 plate displays a contact angle about 60°. In fact, most types of stainless steels are intrinsically hydrophilic because their large surface free energy attracts polar water molecules to chemisorb on the surface. On the contrary, contact angles of all carbon-coated specimens are higher than 100°. Their hydrophobicity arises from non-polar carbon structures, which repels polar water droplet to form a spherical shape so as to lessen the interface area between water droplet and specimen surface. 690 °C-prepared specimen even displays super-hydrophobic surface on which water droplets are unable to adhere. We hence enlarged volume of water droplet until it just dropped out from the buret. This spherical droplet is deformed by its self-weight, but it forms a very large contact angle in excess of 140° and shows almost no hysteresis, allowing itself to easily roll off the surface. We propose that the super-hydrophobicity of 690 °C-prepared specimen is in accordance with the so-called "Lotus Effect" [23,24] due to its micrometer-sized rough surface composed of nanometer-sized carbon filaments.

810 °C-prepared carbon film is obviously more hydrophobic than 930 °C-prepared one. Contact angle of the former (120°) is even higher than that of HOPG (107°). Although graphite is most hydrophobic in all carbon phases [25,26], the determinants of hydrophobicity of resultant carbon films go beyond their degree of graphitic ordering. Earlier studies pointed out that surface free energy of carbon film substantially diminishes after hydrogenation as a result of the formation of C–H bonds by saturating dangling carbon bonds [27–31]. Since our specimens are CVD-processed under a hydrogen-containing atmosphere, it is reasonable to deem that the formation of C–H bond takes place on the surface of resultant carbon films. Although 810 °C-prepared carbon film is amorphous, C–C sp^3-bonding provides much more surface dangling bonds to form C–H bonding. This effect makes the hydrophobicity of 810 °C-prepared carbon film superior to that of HOPG. On the other hand, the inferior hydrophobicity of 930 °C-prepared carbon film is ascribed to its graphitic structure and small coherency. The former provides much lesser dangling bonds for the formation of C–H bonds; the latter usually signifies numerous grain boundaries on the film surface, both induce relatively higher surface energy.

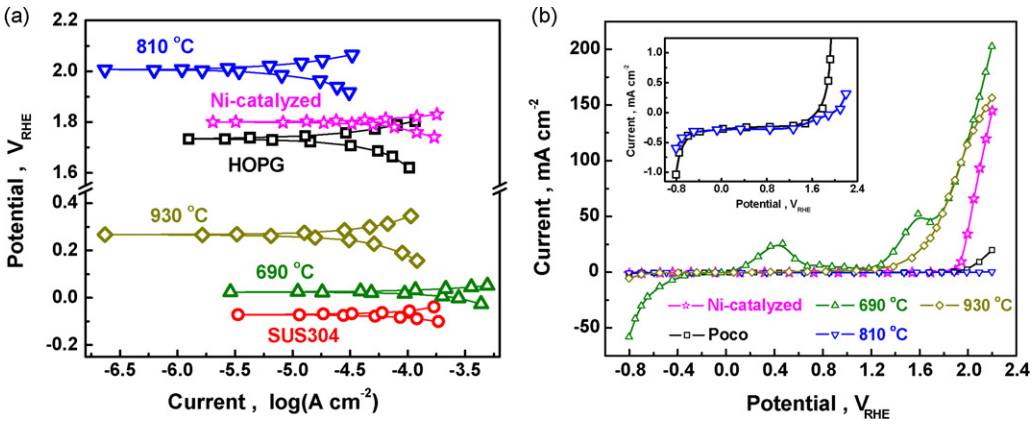

Fig. 6. (a) Tafel plot and (b) *C–V* curves of the specimens investigated. Specimens were tested in 0.5 M H_2SO_4 solution at 25 °C.

3.5. Electrochemical stability

Studies of metallic bipolar plate are usually focused on corrosion behaviours in PEMFC anode. Recently, many reports indicated that PEMFC cathode is favourable for the oxidation of carbon support to CO_2, i.e. carbon is corroded severely in an environment with the presence of O_2, liquid water, and potential over 0.6 V_{RHE} [32–34]. To explore whether our carbon films can protect SUS304 substrate against corrosion in PEMFC anode and moreover prevent themselves from gasification in PEMFC cathode, specimens were subjected to potentiodynamic polarization test in 0.5 M H_2SO_4 solution to simulate accelerated corrosion conditions in PEMFC. Fig. 6(a) and (b) individually shows Tafel plot and *C–V* curves of the specimens investigated. Corrosion potentials in Tafel plot and reaction current densities in *C–V* curves are the criteria used to assess the electrochemical stabilities of specimen investigated in this study. Thermodynamically, higher (noble) corrosion potential in Tafel plot means better electrochemical stability of the specimen. The corrosion potentials of materials used as bipolar plates (anodic and cathodic sides) of PEMFC should be higher than 0 or 1.23 V_{RHE}, respectively, to prevent themselves from corrosion (anode side) or gasification by oxidation (cathode side). Reaction current densities in *C–V* curves kinetically correspond to dissolution rates of specimens, i.e. lower anodic current density means better durability of the specimen in PEMFC environment. 690 °C-prepared specimen displays a corrosion potential just slightly higher than that of bare SUS304 (0.03 vs.−0.07 V_{RHE}). Its *C–V* curve shows relatively severer reaction current density with the appearance of two redoxs at around 0.4 and 1.6 V_{RHE}, which are also observed on bare SUS304 plate, indicating that the film composed of carbon filaments is apparently unable to provide complete protection to SUS304 substrate. By contrast, specimens with continuous carbon film structure perform much better in chemical stability. Although 930 °C-prepared specimen displays a corrosion potential at 0.27 V_{RHE}, its *C–V* curve indicates the fact that corrosion is in fact slight until potential is higher than 1.20 V_{RHE}.

810 °C-prepared specimen, impressively, reveals a corrosion potential approaching as high as 2.01 V_{RHE}, which is even higher than that of HOPG (1.73 V_{RHE}). *C–V* curve of 810 °C-prepared specimen further demonstrates that its reaction current is actually hardly detectable in the investigated range of potentials, as compared with the other specimens. The inset in Fig. 6(b) shows detailed information about the *C–V* curves of HOPG and 810 °C-prepared specimen. Apparently, 810 °C-prepared specimen not only performs better than HOPG in chemical inertness, but its dissolution rate is also much less than that of HOPG in high potential region (0.31 mA cm^{-2} vs. 19.6 mA cm^{-2}, at V_{RHE} 2.20), meaning

Table 1
Concentrations of metal ions in H_2SO_4 solutions after potentiodynamic polarization tests.

Specimen (corrosion potential)	Element\concentration (ppm)		
	Fe	Cr	Ni
SUS304 (at −0.07 V_{RHE})	8.18	1.58	1.73
690 °C-prepared specimen (at 0.03 V_{RHE})	4.24	1.25	0.449
810 °C-prepared specimen (at 2.01 V_{RHE})	Nil	Nil	Nil
930 °C-prepared specimen (at 0.27 V_{RHE})	1.47	0.392	Nil
Detection limit (ppb)	3.8	3.1	3.8

it is almost non-reactive with $H_{(aq)}^+$ and O_2. The optimal carbon film deposited on Ni-coated SUS304 plate, i.e. Ni-catalyzed carbon film, also exhibits superior chemical inertness, showing corrosion potential at 1.80 V_{RHE}, see also Fig. 6(a). However its anodic current increases as the potential is higher than +1.80 V_{RHE}. At 2.20 V_{RHE} the anodic current reaches 145 mA cm^{-2}, which is almost 500 times that of 810 °C-prepared specimen. This implies that gasification of Ni-catalyzed carbon film at high potential is quite severe and/or a significant dissolution of nickel occurs in the same potential domain. Therefore SUS304 bipolar plate coated with 810 °C-prepared carbon film is much more durable than that coated with Ni-catalyzed carbon film in PEMFC environment.

After potentiodynamic polarization tests, concentrations of metal ions in H_2SO_4 solutions were measured, as listed in Table 1. The amount of metal ions dissolving in H_2SO_4 solutions reduces with increasing corrosion potential of specimens. Corrosion on carbon-coated SUS304 substrate prepared at 690 °C and 930 °C is evidently lower in comparison to that of bare SUS304 plate. However these two carbon coatings provide insufficient protection as comparing to the case of 810 °C-prepared specimen. In the later case the content of metal ions in H_2SO_4 solution is lower than the detection limit (in terms of ppb), indicating that this carbon coating can fully protect SUS304 substrate against corrosion. We suspect that the excellent chemical stability of 810 °C-prepared specimen is due to the fact that the film surface is filled with C–H bonds induced by hydrogenation in amorphous carbon, forming a protective layer full of hydrogen.

4. Conclusions

We successfully integrate advantages of graphite and metallic plates through a much simplified depositing process of carbon films, without a nickel catalytic layer, onto SUS304 stainless steel plates using a CVD method under gas-mixture of C_2H_2–H_2. Reaction temperature in the CVD process (T_{CVD}) much affects surface

morphology and crystal structure of resultant carbon film. At T_{CVD} around 690 °C the resultant carbon film is mainly composed of carbon filaments whose structures are similar to carbon nano-tubes. As T_{CVD} is higher than 810 °C, continuous film structure forms by the accumulation of carbon spheres, and the resultant carbon film becomes more graphitic with increasing T_{CVD}. All carbon films investigated in this study show substantially improved ICR and hydrophobicity of SUS304 plate to a level comparable to HOPG. The specimen prepared at T_{CVD} 810 °C exhibits superior chemical stability better than that of HOPG and Ni-catalyzed carbon coating. The reason is attributed to the C–C sp^3-bonding of amorphous carbon which provides dangling bonds to form C–H bonding on the surface during hydrogenation. The surface being full of C–H bonds is not merely much more protective against the attack of $H_{(aq)}^+$ at low reaction potential (anodic side) but also suppressing gasification of carbon at high reaction potential (cathodic side).

The superior properties of carbon-coated SUS304 plates by such a simplified method without a Ni-catalytic layer disclose a new aspect for the surface modification of metallic bipolar plate. The use of such carbon-coated SUS304 plates as bipolar plates of PEMFC is expected to reduce the volume while improving the performance of PEMFC. The authors believe the disclosure of our carbon-coated SUS304 plate may further accelerate commercialization of PEMFC.

Acknowledgments

This work was sponsored by National Science Council of Republic of China under Grant No. NSC 95-2218-E-035-005, and by Ministry of Economic Affairs of Republic of China under Grant No. 97-EC-17-A-08-S1-099.

References

[1] S. Gottesfeld, T.A. Zawodzinski, Adv. Electrochem. Sci. Eng. 5 (1997) 195.
[2] Isa Bar-On, R. Kirchain, R. Roth, J. Power Sources 109 (2002) 71.
[3] E.A. Cho, U.-S. Jeon, H.Y. Ha, S.-A. Hong, I.-H. Oh, J. Power Sources 125 (2004) 178.
[4] R. Blunk, M.H.A. Elhamid, D. Lisi, Y. Mikhail, J. Power Sources 156 (2006) 151.
[5] J. Wind, R. Spah, W. Kaiser, G. Bohm, J. Power Sources 105 (2002) 256.
[6] A. Pozio, R.F. Silva, M. De Francesco, L. Giorgi, Electrochim. Acta 48 (2003) 1543.
[7] H. Wang, M.A. Sweikart, J.A. Turner, J. Power Sources 115 (2003) 243.
[8] E.A. Cho, U.-S. Jeon, et al., J. Power Sources 142 (2005) 177.
[9] Y. Sone, H. Kishida, M. Kobayashi, et al., J. Power Sources 86 (2000) 334.
[10] T. Fukutsuka, T. Yamaguchi, S. Miyano, Y. Matsuo, Y. Sugie, Z. Ogumi, J. Power Sources 174 (2007) 199.
[11] Yoshiyuki Show, Surf. Coat. Technol. 202 (2007) 1252.
[12] C.Y. Chung, S.K. Chen, P.J. Chiu, M.H. Chang, T.T. Hung, T.H. Ko, J. Power Sources 176 (2008) 276.
[13] H. March, A.P. Warburton, J. Appl. Chem. 20 (1970) 133.
[14] A.I. Boronin, V.I. Bukhtiyarov, R. Kvon, V.V. Chesnokov, R.A. Buyanov, Surf. Sci. 258 (1991) 289.
[15] C.M. Chun, J.D. Mumford, T.A. Ramanarayanan, J. Electrochem. Soc. 147 (2000) 3680.
[16] C.M. Chun, J.D. Mumford, T.A. Ramanarayanan, J. Electrochem. Soc. 149 (2002) B348.
[17] G.G. Tibbetts, J. Cryst. Growth 66 (1984) 632.
[18] M. Inagaki, Solid State Ionics 86–88 (1996) 833.
[19] M. Inagaki, Carbon 5 (1997) 711.
[20] R.F. Silva, D. Franchi, A. Leone, L. Pilloni, A. Masci, A. Pozio, Electrochim. Acta 51 (2006) 3592.
[21] R.F. Silva, A. Pozio, J. Fuel Cell Sci. Technol. 4 (2007) 116.
[22] P. Zhou, C.W. Wu, G.J. Ma, J. Power Sources 159 (2006) 1115.
[23] C. Neinhuis, W. Barthlott, Ann. Bot. 79 (1997) 667.
[24] L. Feng, S. Li, Y. Li, H. Li, L. Zhang, J. Zhai, Y. Song, B. Liu, L. Jiang, D. Zhu, Adv. Mater. 14 (2002) 1857.
[25] L. Ostrovskaya, V. Perevertailo, V. Ralchenko, A. Dementjev, O. Loginova, Diamond Relat. Mater. 11 (2002) 845.
[26] T. Werder, J.H. Walther, R.L. Jaffe, T. Halicioglu, P.J. Koumoutsakos, J. Phys. Chem. B 107 (2003) 1345.
[27] T. Halicioglu, Surf. Sci. Lett. 259 (1991) L714.
[28] G. Kern, J. Hafner, G. Kresse, Surf. Sci. 366 (1996) 464.
[29] Y.M. Wang, K.W. Wong, S.T. Lee, M. Nishitani-Gamo, I. Sakaguchi, K.P. Loh, T. Ando, Diamond Relat. Mater. 9 (2000) 1582.
[30] V.G. Aleshin, A.A. Smekhnov, G.P. Bogatyreva, V.B. Kruk, Chemistry of Diamond Surface, Naukova Dumka, Kiev, 1990, p. 200 (in Russian).
[31] J.B. Cui, J. Ristein, L. Ley, Phys. Rev. B 60 (1999) 16135.
[32] C.A. Reiser, L. Bregoli, T.W. Patterson, J.S. Yi, J.D. Yang, M.L. Perry, T.D. Jarvi, Electrochem. Solid-State Lett. 8 (2005) A273.
[33] L.M. Roen, C.H. Paik, T.D. Jarvi, Electrochem. Solid-State Lett. 7 (2004) A19.
[34] K. Kangasniemi, D. Condit, T.D. Jarvi, J. Electrochem. Soc. 151 (2004) E125.